Referee general comment*: This article aims to reconstruct past hydrological regimes and the evolution of the Southern Westerly Wind (SWW) belt since the Last Glacial Maximum, based on hydrogen isotope ratios of leaf-wax n-alkanes in marine sediments between 33°S and 36°S. Past variations in the SWWs (latitudinal shifts, intensity, timing) remain a subject of debate, making this study highly relevant to the scientific community. Equally important is its examination of SWW–South Pacific High (SPH) interactions and their links to tropical dynamics.*

The manuscript is interesting and well-structured. While the methodology is not entirely novel, it is noteworthy in that it has not previously been applied to this region of the southwest coast of South America for these purposes. The results are thoroughly analyzed, and the interpretations are convincing.

One aspect that I found slightly confusing was the frequent reference to previously published data and/or databases, such as those by Läuchli et al. (2025; note: this reference is incomplete in the reference list) and Gaviria-Lugo et al. (2023a, b). While this does not affect the overall quality of the work, clearer integration of these sources would improve the manuscript's readability.

We thank the Anonymous Referee #2 for the review and the constructive comments. The modifications made to the manuscript in response to the comments of Anonymous Referee #2 are described in this document. Briefly, references to database and/or published data were clarified and minor comments were addressed.

In this document, the comments of the Anonymous Referee #2 are indicated in *italic* and our answers are indicated in normal or bold fonts with bullet points. Modification performed to the manuscript are indicated in bold in the tables.

References to published data and/or database

One aspect that I found slightly confusing was the frequent reference to previously published data and/or databases, such as those by Läuchli et al. (2025; note: this reference is incomplete in the reference list) and Gaviria-Lugo et al. (2023a, b). While this does not affect the overall quality of the work, clearer integration of these sources would improve the manuscript's readability.

- To address the Referee's comment, we try to integrate in a clearer way citations to data publications. Note that the data associated with this article are reported in a data publication following the requirements of CP as well as FAIR principles. The reference to Läuchli et al. 2025 will be updated and made publicly available by acceptance of the article. The reference to the data publication will then be modified.
- In order to clarify the references to the data publication, "reported in" was added to most references to the tables reported in Läuchli et al. 2025. Furthermore, the tables in the data publication were renamed as Table 5 instead of Table S5.
- Here, we provide some examples:

Old	New
Hydrogen isotope composition (n-C31) of modern fluvial sediments (green, Gaviria-Lugo et al., 2023a, b), marine surface sediments (MUC, light blue, Gaviria-Lugo et al., 2023a, b) and gravity cores (Ln. 95-96)	(c) Hydrogen isotope composition (n-C_{31}) of modern fluvial sediments **(green, Gaviria-Lugo et al., 2023a**), marine surface sediments (MUC, light blue, **Gaviria-Lugo et al.**, **2023a**) and gravity cores […]
δ13C values reported in Tables S5 to S7 (Läuchli et al., 2025, see Data availability). (Ln. 104)	$\delta^{13}C$ values reported in Tables 5 to 7 **reported in Läuchli et al. (2025, see Data availability)**

We preferred previously published ages acquired on planktic foraminifera samples over benthic foraminifera samples for core sections with a high density of radiocarbon age measurements. (Ln. 226-227)	Note that we preferentially selected previously published ages acquired on planktic foraminifera samples over benthic foraminifera samples for core sections with a high density of radiocarbon age measurements **(Table 1 reported in Läuchli et al., 2025, see Data availability).**
New age-depth models were established for cores GeoB7139-2 (30°S), GeoB3304-5 (33°S) and 22SL (36°S) using previously published and newly acquired radiocarbon ages (Table **S**1 in Läuchli et al., 2025, see Data availability). (Ln. 296)	New age-depth models were established for cores GeoB7139-2 (30°S), GeoB3304-5 (33°S) and 22SL (36°S) using previously published and newly acquired radiocarbon ages (Table **1** in Läuchli et al., 2025, see Data availability).
The reservoir ages and offsets used in each scenario are provided in Table S1(Läuchli et al., 2025, see Data availability). (Ln. 327)	The reservoir ages and offsets used in each scenario are provided in Table **1 reported in Läuchli et al. (2025, see Data availability).**
The modelled sediment ages span 36 and 1 ka BP (Scenarios 1 and 2, Table S2 in Läuchli et al., 2025, see Data availability) for site GeoB7139-2, and up to about 24 ka BP and 20 ka BP for sites GeoB3304-5 and 22SL, respectively (Scenarios 1 and 2, Tables S3 and S4 in Läuchli et al., 2025, see Data availability). The differences between the two scenarios modelled are reported in the Tables S2 to S4 (Läuchli et al., 2025, see Data availability). (Ln 329-335)	The modelled sediment ages span 36 and 1 ka BP **(Scenarios 1 and 2, Table 2 reported in Läuchli et al., 2025, see Data availability)** for site GeoB7139-2, and up to about 24 ka BP and 20 ka BP for sites GeoB3304-5 and 22SL, **respectively (Scenarios 1 and 2, Tables 3 and 4 reported in Läuchli et al., 2025, see Data availability)**. The differences between the two scenarios modelled are reported in the Tables 2 to 4 reported in Läuchli et al. (2025, see Data availability).
For sites GeoB7139-2 and GeoB3304-5, the largest differences inferred for the two scenarios during the last 25 kyr were approximately 900 years (Tables S2 and S3 in Läuchli et al., 2025, see Data availability). (Ln. 334)	For sites GeoB7139-2 and GeoB3304-5, the largest differences inferred for the two scenarios during the last 25 kyr were approximately 900 years (Tables **2 and 3** in Läuchli et al., 2025, see Data availability).
The abundance and distribution of *n*-alkanes in samples from sites GeoB3304-5 and 22SL are reported in Tables S5 and S6 (Läuchli et al., 2025, see Data availability). (Ln 342)	The abundance and distribution of *n*-alkanes in samples from sites GeoB3304-5 and 22SL are reported in **Tables 5 and 6 reported in Läuchli et al. (2025, see Data availability)**.
The carbon isotope ratios (δ13Cwax) of leaf-wax *n*-alkanes in fluvial sediments, corrected for the pre-industrial carbon isotope composition of the atmosphere, ranged from -34.6 to -26.8‰ (*n*-C31) and -34.2 to -27.1 ‰ (*n*-C29, Fig. 1d, Table S7 in Läuchli et al., 2025, see Data availability). The δ13Cwax of marine surface sediments, corrected for the pre-365 industrial carbon isotope composition of the atmosphere, ranged from -34 to -29.9‰ (*n*-C31) and -33.6 to -29.3‰ (*n*-C29, Fig. 1d, Table S7 in Läuchli et al., 2025, see Data availability). (Ln 363-367)	The carbon isotope ratios ($\delta^{13}C_{wax}$) of leaf-wax *n*-alkanes in fluvial sediments, corrected for the pre-industrial carbon isotope composition of the atmosphere, ranged from -34.6 to -26.8‰ (*n*-C_{31}) and -34.2 to -27.1 ‰ (*n*-C_{29}, Fig. 1d, **Table 7 reported in Läuchli et al., 2025, see Data availability).** The $\delta^{13}C_{wax}$ of marine surface sediments, corrected for the pre-industrial carbon isotope composition of the atmosphere, ranged from -34 to -29.9‰ (*n*-C_{31}) and -33.6 to -29.3‰ (*n*-C_{29}, Fig. 1d, **Table 7 reported in Läuchli et al., 2025, see Data availability).**
Catchment-averaged δ^2H_{precip} values are shown in Fig. 3 and reported in Table S8 (Läuchli et al., 2025, see Data availability). The modern mean annual catchment-averaged δ2Hprecip values ranged between ca. -103 and -44‰. Modern mean catchment-averaged δ^2H_{precip} values ranged between -104 and -23 ‰ for January and between -105 and -28‰ for July. The modern mean catchment-averaged temperature and precipitation amounts are reported in Table S8 (Läuchli et al., 2025, see Data availability). (Ln. 375-379)	Catchment-averaged δ^2H_{precip} values are shown in Fig. 3 and reported in **Table 8 reported in Läuchli et al. (2025, see Data availability)**. The modern mean annual catchment-averaged δ^2H_{precip} values ranged between ca. -103 and -44‰. Modern mean catchment-averaged δ^2H_{precip} values ranged between -104 and -23 ‰ for January and between -105 and -28‰ for July. The modern mean catchment-averaged temperature and precipitation amounts are reported in **Table 8 reported in Läuchli et al. (2025, see Data availability).**

Error bars in (l) represent two standard deviations (2σ) calculated from the values reported in Tables S5 and S6 (Läuchli et al., 2025, see Data availability). [Legend figure 5]	Error bars in (l) represent two standard deviations (2σ) calculated from the values reported in **Tables 5 and 6 reported in Läuchli et** al. (2025, see Data availability).

- Regarding the references to the data discussed in Gaviria-Lugo et al. 2023a and reported in Gaviria-Lugo et al., 2023b, we decided to cite only the scientific article, when referring to this data sets. In order to still provide a reference to the data publication, the lines 113 and 114 were reformulated as follows:

Old (Ln 113)	New
The dataset reported is Gaviria-Lugo et al. (2023a, b) is composed of fluvial and marine surface sediments.	The data set reported **in** Gaviria-Lugo et al. (2023a) **and the associated data publication (Gaviria-Lugo et al., 2023b)** is composed of fluvial and marine surface sediments.

Minor comments

L39: *Clarify what is meant by "modern components" of the SWW and the ITCZ.*

Old (Ln. 39-42)	New
The modern components of the SWW and the ITCZ are relatively well understood (e.g., Garreaud, 2009; Garreaud et al., 2009) and several studies have investigated their past evolution (e.g., Arbuszewski et al., 2013; Haug et al., 2001b; Kaiser et al., 2024; Lamy et al., 2001; Sachs et al., 2009), yet forcing mechanisms and especially dynamic feedbacks between these systems remain debated.	The modern components of the SWW and the ITCZ – **that is seasonal changes in their position and/or their response to climate phenomena such as the El Niño–Southern Oscillation (ENSO) –** are relatively well understood (e.g., Garreaud, 2009; Garreaud et al., 2009) and several studies have investigated their past evolution (e.g., Arbuszewski et al., 2013; Haug et al., 2001b; Kaiser et al., 2024; Lamy et al., 2001; Sachs et al., 2009), yet forcing mechanisms and especially dynamic feedbacks between these systems remain debated.

L158: *The text states the SWW are centered at 50°S, but this is not reflected in Figure 2.*

The latitude of the SWW core during the austral summer was modified in Figure 2.

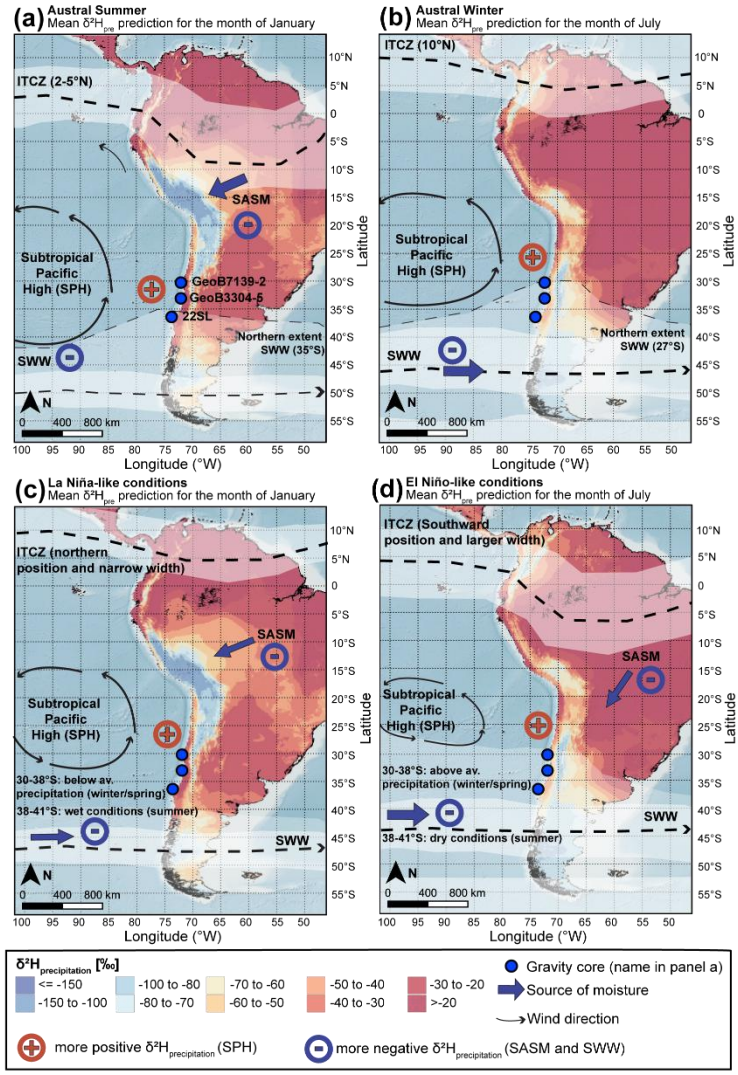

L214: *"Approximately 50 g of fine hemipelagic sediments were sampled." Is 50 g correct?*

- Yes, we sampled 50 g of hemipelagic sedimetns for radiocarbon analysis.

L230: *Briefly describe the two scenarios considered.*

- The previous Lines 278-279 were moved to this paragraph:

Old Ln 230	New
The age-depth models were generated using the BACON v3.2.0 Bayesian age-depth model algorithm developed by Blauuw and Christen (2011). Abrupt changes in sediment accumulation rates as well as turbidites were integrated in the models. To consider the complex ventilation history of the water masses along Chile, two different scenarios were modelled for each site (Sect. 4.1). The parameters used for each BACON age-depth model are detailed in Figs. S2 to S7 reported in the Supplementary Material.	The age-depth models were generated using the BACON v3.2.0 Bayesian age-depth model algorithm developed by Blauuw and Christen (2011). Abrupt changes in sediment accumulation rates as well as turbidites were integrated in the models. To consider the complex ventilation history of the water masses along Chile, two different scenarios were modelled for each site. **In the first scenario, we use reservoir ages from offshore Chile combined with the atmospheric SHCal20 calibration curve (Hogg et al., 2020), while in the second scenario, we directly use the Marine20 calibration curve (Heaton et al., 2020) with local corrections to the global ocean reservoir. Further details are given in Section 4.1.** The parameters used for each BACON age-depth model are detailed in Figs. **S3** to **S8** reported in the Supplementary Material.

L235: *Provide a short explanation of the methodology used by Gaviria-Lugo et al. (2023a).*

- Since the same method was applied to Gaviria Lugo et al (2023) as reported here, the manuscript was modified as follows:

Old Ln 235	New
The lipid extraction method of the modern river and marine surface sediments for which carbon isotope measurements are reported here can be found in Gaviria-Lugo et al. (2023a). For the marine hemipelagic sediments of sites GeoB3304-5 and 22SL, […]	The lipid extraction method of the modern river and marine surface sediments for which carbon isotope measurements are reported here **follow the method described in this study (see below). Details regarding calibration settings** can be found in Gaviria-Lugo et al. (2023a).

L272: *Add the ‰ symbol after "-8.4."*

Old Ln 272	New
-8.4	-8.4 ‰

L278–279: *The first two sentences could be removed without loss of clarity.*

- The two first sentence were deleted.

L300–302: *The description beginning "In the first scenario…" belongs in the methodology section.*

- See answer **L230**